
LLaMP: LARGE LANGUAGE MODEL MADE POWERFUL FOR HIGH-FIDELITY MATERIALS KNOWLEDGE RETRIEVAL AND DISTILLATION

Yuan Chiang^{1,2*}, Chia-Hong Chou³, Janosh Riebesell^{2,4}

¹University of California, Berkeley, ²Lawrence Berkeley National Laboratory,

³Foothill College, ⁴Cambridge University

ABSTRACT

Reducing hallucination of Large Language Models (LLMs) is imperative for use in the sciences where reproducibility is crucial. However, LLMs inherently lack long-term memory, making it a nontrivial, *ad hoc*, and inevitably biased task to fine-tune them on domain-specific literature and data. Here we introduce LLaMP¹, a multimodal retrieval-augmented generation (RAG) framework of multiple data-aware reasoning-and-acting (ReAct) agents that dynamically interact with computational and experimental data on Materials Project (MP). Without fine-tuning, LLaMP demonstrates an ability to comprehend and integrate various modalities of materials science concepts, fetch relevant data stores on the fly, process higher-order data (such as crystal structures and elastic tensors), and summarize multi-step procedures for solid-state synthesis. We show that LLaMP effectively shifts the predictions or corrects the errors of GPT-3.5 intrinsic knowledge, counteracting a 5.21% MAPE of GPT-3.5 on frequently-documented bandgaps and a significant 1103.54% MAPE on formation energies—errors that GPT-3.5 seems to derive from mixed data sources. Additionally, LLaMP substantially reduces the hallucinated volumetric strain in a diamond cubic silicon structure from 66.3% to 0. The proposed framework offers an intuitive and nearly hallucination-free approach to exploring materials informatics and establishes a pathway for knowledge distillation and fine-tuning other language models. We envision the framework as a valuable component for scientific hypotheses and a foundation for future autonomous laboratories where multiple LLM agents communicate and cooperate with robotics to drive material synthesis and chemical reactions without hard-coded human logic and intervention.

1 INTRODUCTION

On the recent development of large language models (LLMs), the generation of convincing yet unreliable information poses a pressing challenge. LLMs are prone to hallucination - providing misleading or outright false information with seemingly high confidence (Bang et al., 2023). This issue is particularly concerning for knowledge-intensive tasks, where users rely on chatbots and other AI systems to provide accurate guidance Lewis et al. (2020). Recent events have underscored how LLMs often lack up-to-date factual knowledge on topics outside their training data, necessitating vigorous verification against trusted external sources (Mallen et al., 2023).

The challenge extends to the archive and retrieval of factual knowledge. Much like the alchemists of old, scientists nowadays also grapple with a complex amalgamation of insights and inaccuracies. A notable example is the whirlwind surrounding copper-substituted lead phosphate apatite (LK-99) as a room-temperature ambient superconductor (Laperche et al., 1997; Lee et al., 2023a;b; Griffin, 2023). The scenario underscores the pressing need to validate information effectively and efficiently over structured and unstructured data. Furthermore, in the era marked by the escalating capabilities of generative models, the deployment of untestable and irreproducible LLMs for high-stakes tasks,

*Correspondence to: cyrusyc@berkeley.edu

¹Code and live demo will be available at <https://github.com/chiang-yuan/llamp>.

particularly in scientific and engineering applications, is on the rise. This trend accentuates the importance of scrutinizing and ensuring the reliability of information sources.

Many of the current LLM applications for domain-specific knowledge rely on the fine-tuning of pre-trained LLMs (Gupta et al., 2022; Dunn et al., 2022) or tailored prompt engineering techniques (Yang et al., 2023; Zheng et al., 2023b). While these models are easy to deploy, they suffer from diminished reproducibility and data adherence due to the absence of a memory base, untraceable fine-tuning history, or opaque extraction processes. Even though fine-tuning can encode a certain amount of domain-specific knowledge into LLMs, it is constrained by scalability and intrinsic memory capacity limitations. Fine-tuned LLMs struggle to retain in the long term the knowledge they were trained on as the training progresses, nor can they be aware of the up-to-date events and data beyond pretraining. Tailored prompt messages, while effective, also compromise the generalizability, thus limiting the overall power and flexibility of LLMs. Therefore, a more sensible approach involves equipping LLMs with external memory storage and knowledge databases, allowing them to generate holistic responses via few-shot adaptation to the accessible data and factual information (Lewis et al., 2020).

In this work, we implement a multimodal retrieval-augmented generation (RAG) framework LLaMP to connect LLMs with multiple Materials Project (MP) API endpoints using LangChain (Lewis et al., 2020; Chase, 2022). The framework serves as a safeguard against LLM hallucination and grounds them on high-fidelity material informatics derived from various sources, including computational data from quantum-mechanical first-principles calculations and expert-curated material synthesis recipes (Kononova et al., 2019). Through hierarchical planning of multiple reasoning-and-acting (ReAct) agents (Yao et al., 2023), we demonstrate that LLaMP not only correctly retrieves higher-order material data such as tensors and crystal structures but also combines different modalities for complex, knowledge-intensive inferences and operations. Additionally, we quantify the deviation of LLM intrinsic knowledge from MP data on scalar materials properties and 3D crystal structures, highlighting the importance of data adherence of LLMs in scientific hypotheses and applications.

The remainder of the paper is organized as follows: Section 2 introduces the background of the Materials Project (materialsproject.org) and the utilization of natural language processing in materials informatics; Section 3 provides a review of related work, focusing on material applications; Section 4 introduces our proposed methodology and the LLaMP architecture; Section 5 outlines the experimental setup and results; and finally, in Section 6, we discuss the implications of our findings and propose directions for future research.

2 BACKGROUND

Materials Project (MP) The Materials Project is dedicated to advancing the exploration of advanced materials crucial for sustainable energy and advanced technology (Jain et al., 2013). Leveraging high-throughput computing and the Vienna Ab Initio Simulation Package (VASP) (Kresse & Furthmüller, 1996), the initiative employs density functional theory (DFT) for precise assessments of material properties using various exchange-correlational functionals including GGA, GGA+U, r2SCAN, and others. These calculations involve spin polarization with high-spin ferromagnetic initialization, potentially allowing low spin state relaxation (Jain et al., 2011; Ong et al., 2013). Structures selected from the Inorganic Crystal Structure Database (ICSD) undergo standardized relaxation procedures, followed by post-processing or additional calculations for higher-order material properties such as electron and phonon bandgaps, elastic tensors, dielectric tensors, and more.

Natural language processing (NLP) NLP has found extensive application in extracting valuable information from scientific publications, with notable instances involving text-to-text or more recent image-to-text summarization techniques (Tshitoyan et al., 2019; Radford et al., 2021; Gupta et al., 2022). For summarizing crystal structures in textual form, Ganose & Jain (2019) introduced the *robocrystallographer*, a toolkit designed for the analysis and generation of descriptions for crystalline materials. Their method condenses atomic structures into descriptive JSON representations that encompass coordination statistics, connectivity motifs, geometric features, and dimensionality. Multiparagraph human-level descriptions for 130K compounds from the Materials Project were generated and are accessible through the MP website and API (Jain et al., 2013).

Language models (LMs) Recent work has explored scaling language models to billions or trillions of parameters, resulting in models such as GPT-3, GPT-4 (OpenAI, 2023), LLaMA 2 (Touvron et al., 2023), and PaLM (Chowdhery et al., 2022). These models are trained in a self-supervised fashion on extensive text corpora, employing objectives such as auto-regressive next-word prediction. Utilizing the transformer architecture (Vaswani et al., 2023), which incorporates self-attention mechanisms to model long-range dependencies in text, these models learn representations during pre-training that capture semantic and syntactic information about language. The resulting large language models exhibit few-shot generalization abilities on downstream natural language tasks without the need for task-specific fine-tuning. However, when applied to knowledge-intensive tasks, language models show limited capability and often hallucinations (Lewis et al., 2020; Bang et al., 2023).

3 RELATED WORK

Prompting Prompt-based methods have emerged as effective tools for automating the data extraction process from the literature (Polak & Morgan, 2023; Yang et al., 2023). The common approach typically involves one or multiple of the following workflows: (1) Classification, where language models assess whether a paragraph or sentence contains the relevant information (Polak & Morgan, 2023). (2) Summarization, where sentences and paragraphs are distilled or transformed into different formats such as table and JSON (Zheng et al., 2023b). (3) Embedding and indexing, where LLMs transform the extracted data into vector embeddings for downstream filtering or top-K retrieval. (4) Examination, where another or the original LLMs are asked to criticize or evaluate the responses. For examples, Polak & Morgan (2023) employ a prompt workflow to extract the cooling rates of metallic glasses and yield strengths of high entropy alloys. Zheng et al. (2023b) implement a ChatGPT metal-organic framework (MOF) synthesis assistant through embedding and searching on preselected papers. Yang et al. (2023) use GPT-4 to extract experimentally measured bandgaps to train a graph neural network for accurate bandgap prediction from crystal structures.

Despite the success in the specific data extraction tasks, prompt-based methods face challenges in reproducibility when the used prompts are kept closed-source or are fine-grained to work for specific edge cases. They are also less generalizable to combine different modalities and sources due to the deliberately designed prompt messages. Regarding response examination and evaluation, although LLM-as-a-judge is scalable and explainable, it has been shown subject to position, verbosity, and self-enhancement biases (Zheng et al., 2023a). The limited capability of LLMs in math and reasoning also contributes to the difficulties in properly grading the responses, particularly for knowledge intensive tasks in scientific and engineering workflows.

Fine-tuning Several knowledge-grounded, domain-specific language models lean on the fine-tuning approach against pre-selected data and literature. For instance, ChemGPT, proposed by Frey et al. (2022), involves fine-tuning GPT-neo on self-referencing embedded strings (SELFIES) representations of small molecules. Dunn et al. (2022) fine-tuned GPT-3 on ~500 prompt-completion pairs to enhance LLM’s capability to extract useful information on materials chemistry from text paragraphs. However, the fine-tuned models without augmentation inherently lack awareness of recent results and any data only available after their training. Moreover, LLMs suffer from limited memory retention and are prone to forget during continual training (Wang et al., 2023).

An alternative perspective is utilizing fine-tuned models for dataset augmentation or knowledge distillation rather than aiming for exhaustive generality within the constraints of memory capacity and retention. Xie et al. (2023) tuned GPT-3 on the Perovskite solar cell FAIR dataset, employing the model to expand the existing dataset by extracting data from newly published literature. In a different approach, Semnani et al. (2023) introduced WikiChat, a combination of RAG and fine-tuning to distill an open-domain chatbot, alleviating the hallucination problem and improving latency and affordability.

4 LLAMP IMPLEMENTATION

Retrieval-augmented generation (RAG) While LLMs and generative pre-trained transformers have demonstrated the capability to store factual knowledge in model parameters, their ability to accurately access and manipulate precise information is limited (Lewis et al., 2021). Deliberate

prompting does not entirely resolve this problem and, in fact, can make models overly sensitive to input requests and induces serious hallucinations. Addressing these challenges, Lewis et al. (2021) proposed the RAG framework, which significantly mitigates these problems through the retriever-generator paradigm. The original RAG framework has two components: (i) a retriever $p_{\eta}(z|x)$ with parameters η that returns top-K documents given the input text sequence x and (ii) a generator $p_{\theta}(y_i|x, z, y_{1:i-1})$ with parameters θ that generates the current output text sequence y based on the context of input sequence x , the retrieved document z , and the previous output sequences $y_{1:i-1}$ (Lewis et al., 2021). In the context of this work, the retriever and generator are replaced by LLMs, and an intermediate data retrieval step is introduced: API function calls to Materials Project, arXiv, and Wikipedia are executed to retrieve consistent and reliable data, which is then parsed or filtered by LLMs to generate text or JSON responses.

Reasoning and acting (ReAct) One-shot generation often falls short in delivering optimal performance for numerous knowledge-intensive reasoning tasks (e.g. HotpotQA, Fever) (Yao et al., 2023). In an effort to enhance performance, Wei et al. (2023) introduced the chain-of-thought (CoT) framework, which encourages language models to engage in reasoning before generating a response. While successful in boosting performance, CoT is susceptible to hallucinations arising from the generated thoughts (Yao et al., 2023). In this work, we adopt ReAct to augment the agent’s action space \mathcal{A} with a language space \mathcal{L} to create an expanded action space $\hat{\mathcal{A}} = \mathcal{A} \cup \mathcal{L}$. This expanded action space empowers the agent to take action $\hat{a}_t \in \mathcal{L}$ in language space that allows LLMs to reason over context. The action \hat{a}_t functions as a *thought*, synthesizing valuable information by reasoning over the existing context c_t and updating the context $c_{t+1} = (c_t, \hat{a}_t)$ for future actions (Yao et al., 2023). These intermediate reasoning steps play a crucial role in scientific hypotheses and greatly improve the hit rate of LLaMP.

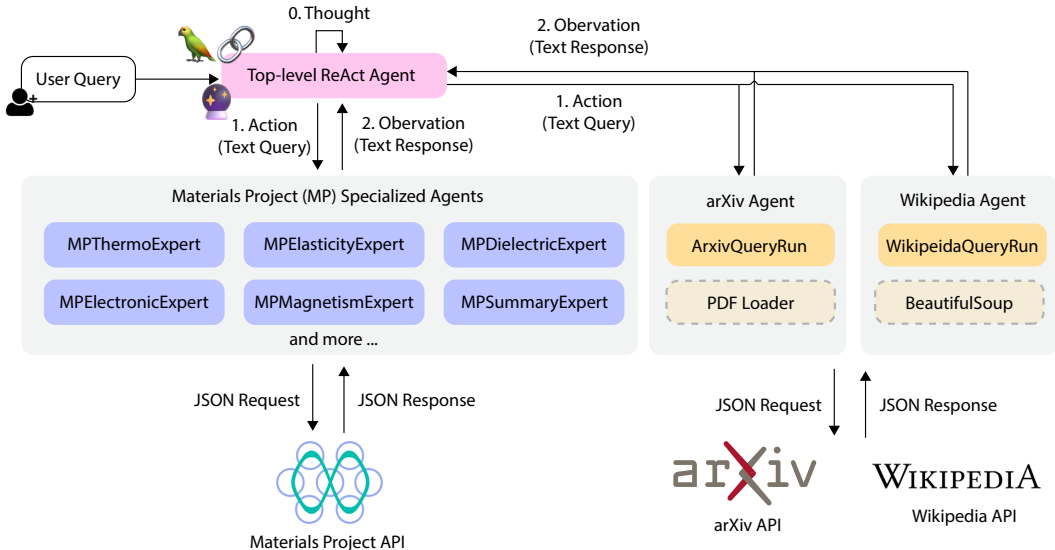


Figure 1: Hierarchical ReAct agent orchestration in LLaMP. Two levels of agents are deployed using a standardized LangChain interface. Top-level ReAct agent oversees assistant ReAct agents at the bottom-level, each equipped with distinct toolkits and data stores. The figure showcases six of the implemented Materials Project (MP) specialized agents. Components represented by dashed lines are excluded from exploration in this paper due to their significant impact on response latency.

Hierarchical orchestration To adeptly manage heterogeneous data sources and diverse types of queries, we introduce hierarchical ReAct agent planning, featuring the top-level ReAct agent overseeing specialized ReAct agents (Figure 1). This design offers three major advantages. Firstly, the top-level agent acts as a router and decision-maker, handling abstract logic between user requests and specialized agents, thereby enhancing the robustness and interpretability of the final response. Secondly, top-level agents can integrate different sources of data parsed via specialized agents, enhancing the completeness of the final response. Thirdly, the process of function calling necessitates LLMs to assimilate API schemas, a task that can impede efficiency by consuming valuable space in

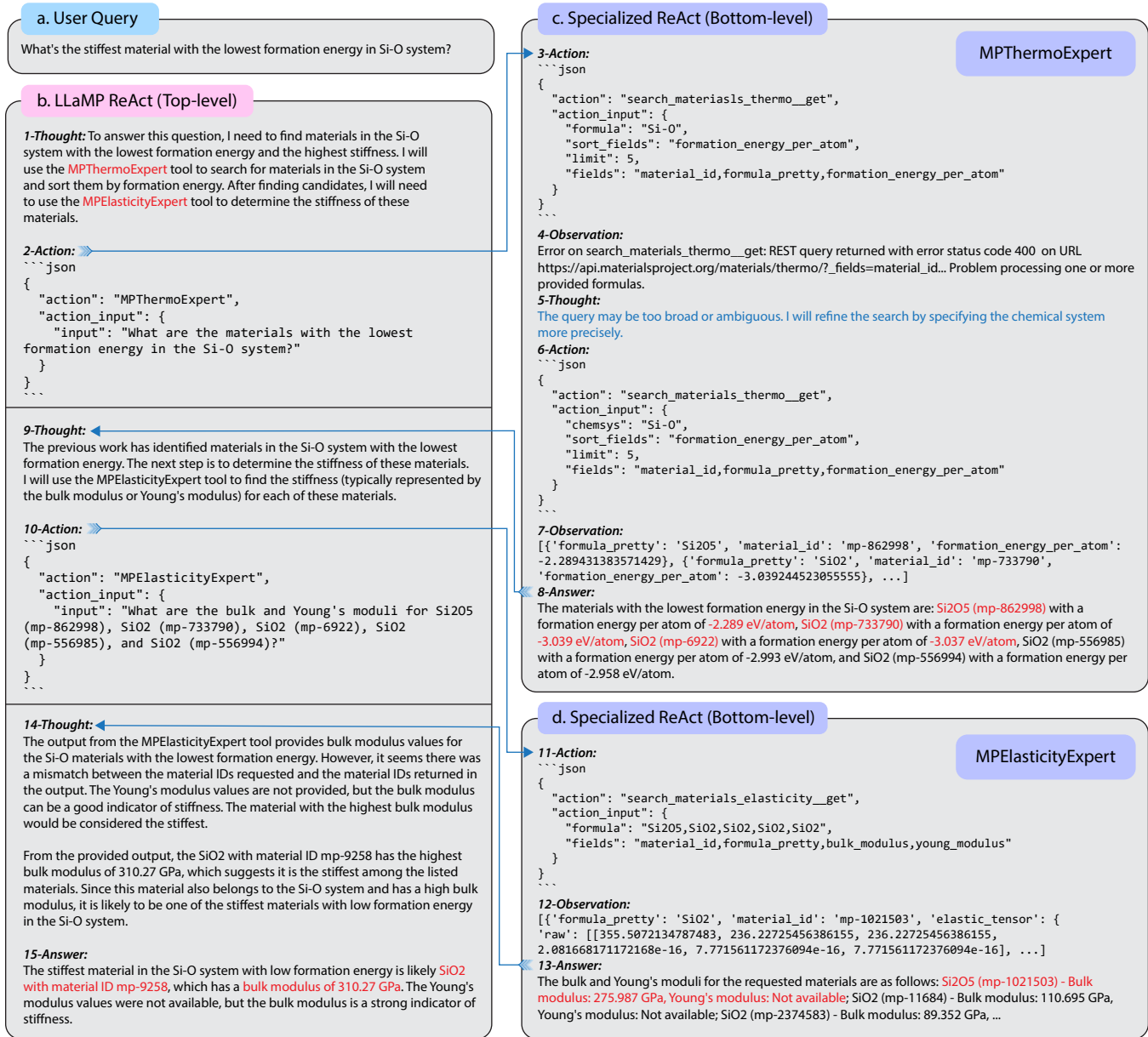


Figure 2: Multimodal retrieval-augmented generation for materials informatics. (a) User query. (b) Top-level ReAct agent capable of handling multiple specialized agents and high-level reasoning for user queries. (c-d) Specialized ReAct agents executing function calling and summarization. (c) **MPThermoExpert** and (d) **MPElasticityExpert** have access to the API schemas of thermo and elasticity endpoints on Materials Project, respectively. The selected details are highlighted in red, demonstrating the capabilities of RAG and ReAct implemented in LLaMP. The blue texts show LLaMP specialized ReAct agent can handle API calling errors and adapt the input query accordingly.

the context window for each question and accelerating the depletion of API tokens. By delegating multiple functions to specialized agents, we effectively reduce the total number of required tokens effectively and circumvent the need for unnecessary schema parsing. Simultaneously, adherence to API schemas is improved since LLMs increasingly struggle to comply if said schemas approach significant fractions of the context window.

5 EXPERIMENTS

Multimodal augmentation Condensed matter physics, inorganic chemistry, and materials engineering frequently involve multifaceted, intricate aspects of materials properties. In many cases, these properties interact in complex ways, with optimizing one factor potentially incurring costs or deterioration in others. For example, dielectric constant usually conflicts with bandgap in materials for electronic devices (Riebesell et al., 2024); and high elastic modulus and low thermal conductivity are hard to achieve simultaneously for thermoelectrics (Musicó et al., 2020). Hence, thoroughly assessing all competing factors and relevant material properties is crucial. Direct interaction with LLMs is unlikely to systematically process different modalities, as engaging in direct conversation with LLMs proves limited in handling compound logic, arithmetic operations, and multiple information sources (Wei et al., 2023).

LLaMP solves the limitation naively through the hierarchical orchestration of multiple ReAct agents (Yao et al., 2023). As illustrated in Figure 2, when presented with a query necessitating multimodal information and compound logic, LLaMP’s top-level agent decomposes the query into multiple sub-tasks and plans to use specialized agents (MPThermoExpert and MPElasticityExpert) for information retrieval. For the example query “What’s the stiffest material with the lowest formation energy in the Si–O chemical space?,” LLaMP strategically dissects this question into two subtasks during its thought process: (i) using MPThermoExpert to search for Si–O materials and (ii) using MPElasticityExpert to assess the stiffness of the retrieved materials. Following this planning phase, the top-level agent orchestrates the retrieval of formation energies (Figure 2c) and elastic moduli (Figure 2d) from the specialized agents. Subsequently, in the final stage of reasoning (step 14 in Figure 2b), the top-level agent integrates information from both modalities, drawing on the context stored in the memory buffer and responses from the specialized agents.

Higher-order and high-fidelity data retrieval The challenge for LLMs in excelling at knowledge- and data-intensive tasks is well-documented. Without RAG, vanilla LLMs often succumb to hallucinations, especially when the tasks involve numerical values or operations, or finding supporting references to the given answer. As shown in Table B3.2, GPT-3.5 hallucinates the values for the components in the elastic tensor of NaCl, with serious erroneous values such as $C_{11} = 289.2$ GPa—a significant deviation from DFT-calculated values (76 GPa). It also omits the values for $C_{22}, C_{33}, C_{55}, C_{66}$ and fails to represent the full elastic tensor in a matrix format, despite the query explicitly requesting the *full* elastic tensor.

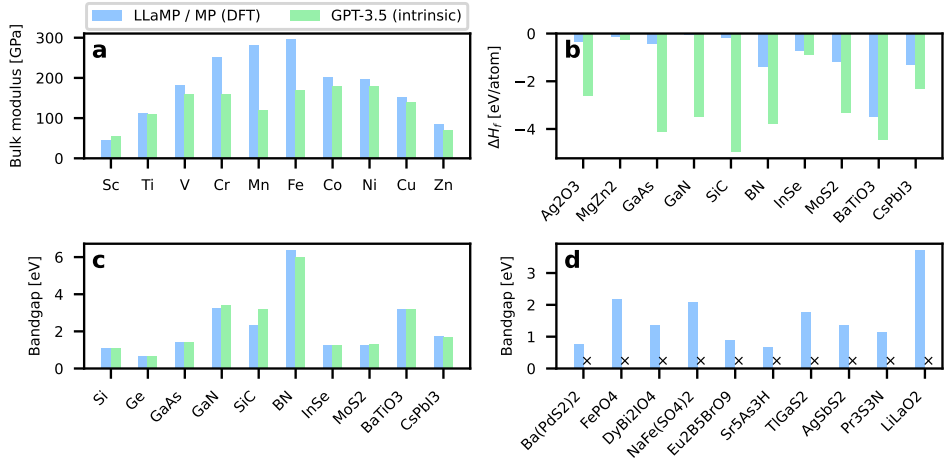


Figure 3: LLaMP RAG responses vs GPT-3.5 intrinsic knowledge on material properties. LLaMP values are identical in all cases to the corresponding data in MP which we treat as ground truth. (a) Bulk moduli, K , of 3d transition metals. (b) Formation energies, ΔH_f , of common compounds. (c) Intrinsic bandgaps, E_g , of common bulk crystals for semiconductors. (d) Intrinsic bandgaps of multi-element (ternary or quaternary) materials. Missing predictions are marked by cross symbols. Mean absolute percentage errors (MAPE) are reported in Table 1.

To underscore the pivotal role of RAG in material informatics applications, we test vanilla GPT-3.5 (without RAG) and LLaMP (with RAG) on queries related to scalar material properties. Figure 3 presents the responses of LLaMP and GPT-3.5 regarding the bulk modulus, formation energy, and bandgap of selected materials. It is noteworthy that GPT-3.5 exhibits surprisingly accurate responses for the bandgaps of common semiconductors² but tends to hallucinate when predicting the formation energies of common compounds and the bulk moduli of certain transition metals (Figure 3, Table 1). This is likely attributable to the extensive literature corpus on experimental and theoretical semiconductor bandgaps, which have been studied and reported for decades due to intense and enduring interest in these materials for electronic devices. In contrast, reliable mechanical tests of materials are often scarce and not easily searchable via text mining.

Without additional prompting, language models overlook the subtleties of domain knowledge and may display overconfidence in intrinsic knowledge, which could be influenced by misleading data that appear more frequently and are more accessible. This is commonly referred to as the “tail knowledge problem” (Kandpal et al., 2023; Liu et al., 2023). To illustrate this, we query LLaMP and GPT-3.5 about the bandgaps of 10 multi-element materials that are less commonly encountered in the literature. As demonstrated in Figure 3d and Table B3.8, GPT-3.5 lacks intrinsic knowledge of the bandgaps for the queried multi-element materials and fails to make predictions, whereas LLaMP could not only correctly retrieve the data but also identify the bandgap of the stable form when multiple polymorphs are present. Additionally, GPT-3.5 severely underestimates formation energies, possibly due to its training corpus being skewed toward molecular rather than crystalline data, as suggested by the use of “kJ/mol”, a more common unit in the molecular chemistry community, in the GPT-3.5 response.

RAG-assisted crystal generation and editing LLMs fine-tuned for text-encoded atomistic information have shown the capability to generate stable crystals under the constraints of atomic positions and charges (Gruver et al., 2023). In this context, we delve into the examination and comparison of the crystal generation capabilities between LLaMP and GPT-3.5, without resorting to fine-tuning or tailored prompt messages in previous work. Figure 4 showcases the structures generated by LLaMP and vanilla GPT-3.5 without RAG, both instructed to *insert one lithium atom at the tetrahedral site of the diamond cubic silicon structure* (Table B3.11). Notably, both LLaMP and GPT-3.5 place an additional Li atom at fractional coordinate (0.5, 0.5, 0.5). However, the Si structure retrieved by LLaMP adheres to the MP convention, positioning two Si bases at (0.125, 0.125, 0.125) and (0.875, 0.875, 0.875). This causes the inserted Li atom to be *hexagonal interstitial* instead of *tetrahedral interstitial*.

GPT-3.5 locates the Li atom at the tetrahedral site given the “luckily chosen” Si bases at (0, 0, 0) and (0.25, 0.25, 0.25); however, the resulting cell volume and shape are highly distorted, and the Si–Si bond length and Si–Si–Si angle deviate significantly from the ground truth (Table 2), highlighting the limitations in the intrinsic encoding of LLMs for atomistic information and the challenges associated with zero-shot generation of crystal structures.

In contrast, the LLaMP-retrieved MP structure serves as a robust prior, anchoring the lattice parameters of the generated structure to the correct values. While one might argue that a fine-tuning campaign could correct the errors of naive generation to some extent, the meaningful applications usually require high-quality, accurate values, and it becomes evident that the performance of vanilla LLMs will degrade sharply when the target composition and structure are out of distribution, as exemplified by the lack of intrinsic knowledge for bandgap for multi-element materials in Figure 3d.

Synthesis recipes and procedures Empowered by the MP synthesis endpoint, LLaMP can extract synthesis recipes and summarize detailed step-by-step procedures grounded on real experimental papers with associated digital object identifier (DOI), as demonstrated in the example queries (Table B3.9 and B3.10). On the other hand, GPT-3.5 gives a seemingly correct and verbose synthesis

Table 1: Mean absolute percentage error (MAPE) of material property extraction from GPT-3.5 intrinsic knowledge in comparison with LLaMP retrieved MP values: (a) bulk moduli K , (b) formation energies ΔH_f , and (c-d) bandgaps E_g . Values are computed from the data in Figure 3.

Property	MAPE (%)
(a) K	21.65
(b) ΔH_f	1103.54
(c) E_g	5.21
(d) E_g	NA

²bandgaps calculated from PBE-GGA functional are known to underestimate the experimental values

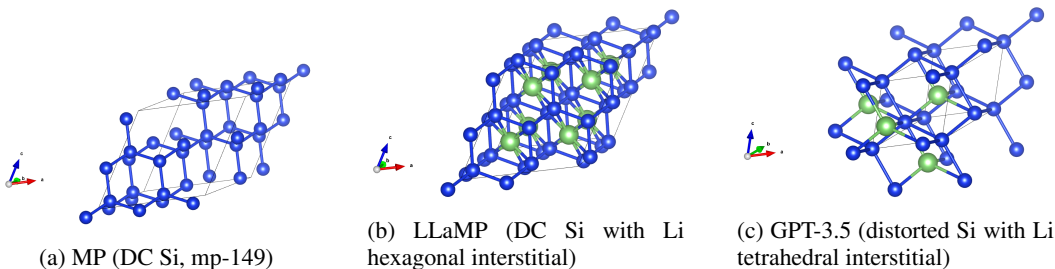


Figure 4: Generate and manipulate crystal structures using LLMs to insert an additional lithium atom at the interstitial site in diamond cubic silicon structure. Blue: Si. Green: Li. Question-answer pairs are listed in Table B3.11. Additional atoms extended through bonds are visualized.

Table 2: Structural parameters of the generated crystals compared with diamond cubic (DC) silicon. From left to right are fractional coordinates of inserted Li atom $(x, y, z)_{\text{Li}}$, total cell volume V , average Si-Si bond lengths ℓ_{SiSi} , Si-Si-Si angles θ_{SiSiSi} , and Si-Li-Si angles θ_{SiLiSi} .

	$(x, y, z)_{\text{Li}}$	ℓ_{SiSi} (Å)	Error (%)	V (Å ³)	Error (%)	θ_{SiSiSi} (°)	Error (%)	θ_{SiLiSi} (°)
LLaMP	(0.5, 0.5, 0.5)	2.36	0.0	40.33	0.0	109.47	0.0	62.96
GPT-3.5	(0.5, 0.5, 0.5)	2.71	+15.0	67.05	+66.3	98.28	-10.2	67.69
DC Si (mp-149)		2.36		40.33		109.47		

procedure for YMnO_3 in Table B3.9, inferring possible reaction pathways from two common oxides as precursors (Y_2O_3 and MnO_2). However, it pulls irrelevant lithium compounds (Li_2CO_3 and LiOH) into the recipe and overlooks the fact that metathesis reactions (Li et al., 2015; Todd et al., 2021) require less applied energy to perform than high-temperature sintering, which relies on solid-state diffusion (Maximenko & Olevsky, 2004). Vanilla GPT-3.5 also exhibits uncertainty about specific synthesis details, such as heating temperature, duration, cooling rate, *etc.*

Consider the example of LiFePO_4 presented in Table B3.10. Explicit instruction is provided: “Please provide a detailed step-by-step procedure and reference”. While GPT-3.5 does offer both a procedure and reference as asked, and the reference is indeed associated with a real paper, the paper itself contains no information about the synthesis procedure of LiFePO_4 . The procedure listed in Table B3.10 is completely hallucinated from the pretraining corpus.

6 DISCUSSION

The implementation of ReAct for the bottom-level agents fortifies the robustness of data retrieval. As presented in Figure 2c, `MPThermoExpert` initially misunderstood the schema at the first trial and filled in the `formula` field with `Si-O`, an invalid input but valid as a chemical system (`chemsys` in the API). The observation step (step 4) allows `MPThermoExpert` to handle exceptions and subsequently generate the correct input fields for MP API endpoints after adaptation (step 6). In future works, storing and retrieving question-answer or query-response pairs from vector databases could reduce the number of trial-and-error steps. Furthermore, the stored pairs can be used to refine foundation LLMs to increase the successful rate of function calling.

LLMs, and recent visual language models (VLMs), have demonstrated the promise to control robotics and guide autonomous chemical experiments (Brohan et al., 2023; Boiko et al., 2023). In the context of self-driving or autonomous laboratory (Boiko et al., 2023; Szymanski et al., 2023), LLM agents must proficiently fetch and manipulate data to support their decision-making and operational tasks. For example, accurate formation energy data calculated from first principles, coupled with correct reaction energy calculations, can aid in identifying viable and faster reaction pathways. The absence of access to a high-fidelity database through autonomous agents like LLaMP would escalate the number of trial-and-error iterations, making the scaling of self-driving laboratory prohibitively expensive and potentially hazardous.

While MP is one of the most comprehensive materials databases, the available crystal structures on MP are not exhaustive but continuously expanding (Merchant et al., 2023). Furthermore, Kohn-Sham DFT theory is insufficient in some cases, and a higher level of theory is needed. One important future direction is to connect with automated high-throughput computational workflows to streamline the process from literature exploration, data extraction, diffusion- or language-based crystal generations (Zeni et al., 2024; Gruver et al., 2023), machine-learned atomistic simulations (Batatia et al., 2023), to high-fidelity computed materials properties.

7 CONCLUSION

We present a hierarchical agentic framework, LLaMP, based on RAG and ReAct to extract and manipulate material informatics through few-shot generalization. By grounding thoughts and actions in high-fidelity information, LLaMP showcases the ability to integrate various modalities of material properties and perform logical inferences to accomplish assigned tasks, all without the need for fine-tuning. In essence, the proposed LangChain framework holds the potential to expand its applicability to multiple data sources, encompassing both theoretical computations and experimental data, and real-world laboratories by incorporating additional assistant agents for data retrieval and robot control. LLaMP functions as a knowledge-aware agent, empowering users to navigate and manipulate complex materials informatics. As new tools continue to emerge, there is an exciting avenue for further exploration to ascertain if this framework can effectively facilitate scientific hypotheses and guide data-driven experiments.

AUTHOR CONTRIBUTIONS

Yuan Chiang led, conceptualized, and designed the project, coded the Python backend and application frontend, and drafted the initial manuscript. Chia-Hong Chou coded the application’s front end. Janosh Riebesell provided technical support on crystal visualization using elementari for the front end and revised the manuscript.

ACKNOWLEDGMENTS

We appreciate the helpful discussion with Dr. Anubhav Jain and Dr. Karlo Berket at LBNL, and the early test and feedback from Dr. Matthew McDermott and Dr. Jordan Burns. Yuan Chiang acknowledges the support and advice from Prof. Mark Asta and the financial support from the Berkeley Fellowship from UC Berkeley and Taiwan-UC Berkeley Fellowship from the Ministry of Education in Taiwan. We also thank OpenAI for granting the API credits.

This work was partly supported by the US Department of Energy, Office of Science, Office of Basic Energy Sciences, Materials Sciences and Engineering Division, under contract no. DE-AC02-05-CH11231 (Materials Project program KC23MP).

REFERENCES

- Yejin Bang, Samuel Cahyawijaya, Nayeon Lee, Wenliang Dai, Dan Su, Bryan Wilie, Holy Lovenia, Ziwei Ji, Tiezheng Yu, Willy Chung, Quyet V. Do, Yan Xu, and Pascale Fung. A Multitask, Multilingual, Multimodal Evaluation of ChatGPT on Reasoning, Hallucination, and Interactivity, November 2023. URL <http://arxiv.org/abs/2302.04023>. arXiv:2302.04023 [cs].
- Ilyes Batatia, Philipp Benner, Yuan Chiang, Alin M. Elena, Dávid P. Kovács, Janosh Riebesell, Xavier R. Advincula, Mark Asta, William J. Baldwin, Noam Bernstein, Arghya Bhowmik, Samuel M. Blau, Vlad Cărare, James P. Darby, Sandip De, Flaviano Della Pia, Volker L. Deringer, Rokas Elijošius, Zakariya El-Machachi, Edvin Fako, Andrea C. Ferrari, Annalena Genreith-Schriever, Janine George, Rhys E. A. Goodall, Clare P. Grey, Shuang Han, Will Handley, Hendrik H. Heenen, Kersti Hermansson, Christian Holm, Jad Jaafar, Stephan Hofmann, Konstantin S. Jakob, Hyunwook Jung, Venkat Kapil, Aaron D. Kaplan, Nima Karimitari, Namu Kroupa, Jolla Kullgren, Matthew C. Kuner, Domantas Kuryla, Guoda Liepuoniute, Johannes T. Margraf, Ioan-Bogdan Magdău, Angelos Michaelides, J. Harry Moore, Aakash A. Naik, Samuel P. Niblett, Sam Walton Norwood, Niamh O’Neill, Christoph Ortner, Kristin A. Persson, Karsten Reuter,

-
- Andrew S. Rosen, Lars L. Schaaf, Christoph Schran, Eric Sivonxay, Tamás K. Stenczel, Viktor Svahn, Christopher Sutton, Cas van der Oord, Eszter Varga-Umbrich, Tejs Vegge, Martin Vondrák, Yangshuai Wang, William C. Witt, Fabian Zills, and Gábor Csányi. A foundation model for atomistic materials chemistry, December 2023. URL <http://arxiv.org/abs/2401.00096>. arXiv:2401.00096 [cond-mat, physics:physics].
- Daniil A. Boiko, Robert MacKnight, Ben Kline, and Gabe Gomes. Autonomous chemical research with large language models. *Nature*, 624(7992):570–578, December 2023. ISSN 1476-4687. doi: 10.1038/s41586-023-06792-0. URL <https://www.nature.com/articles/s41586-023-06792-0>. Number: 7992 Publisher: Nature Publishing Group.
- Anthony Brohan, Noah Brown, Justice Carbajal, Yevgen Chebotar, Xi Chen, Krzysztof Choromanski, Tianli Ding, Danny Driess, Avinava Dubey, Chelsea Finn, Pete Florence, Chuyuan Fu, Montse Gonzalez Arenas, Keerthana Gopalakrishnan, Kehang Han, Karol Hausman, Alexander Herzog, Jasmine Hsu, Brian Ichter, Alex Irpan, Nikhil Joshi, Ryan Julian, Dmitry Kalashnikov, Yuheng Kuang, Isabel Leal, Lisa Lee, Tsang-Wei Edward Lee, Sergey Levine, Yao Lu, Henryk Michalewski, Igor Mordatch, Karl Pertsch, Kanishka Rao, Krista Reymann, Michael Ryoo, Grecia Salazar, Pannag Sanketi, Pierre Sermanet, Jaspier Singh, Anikait Singh, Radu Soricut, Huang Tran, Vincent Vanhoucke, Quan Vuong, Ayzaan Wahid, Stefan Welker, Paul Wohlhart, Jialin Wu, Fei Xia, Ted Xiao, Peng Xu, Sichun Xu, Tianhe Yu, and Brianna Zitkovich. RT-2: Vision-Language-Action Models Transfer Web Knowledge to Robotic Control, July 2023. URL <http://arxiv.org/abs/2307.15818>. arXiv:2307.15818 [cs].
- Harrison Chase. LangChain, October 2022. URL <https://github.com/langchain-ai/langchain>.
- Aakanksha Chowdhery, Sharan Narang, Jacob Devlin, Maarten Bosma, Gaurav Mishra, Adam Roberts, Paul Barham, Hyung Won Chung, Charles Sutton, Sebastian Gehrmann, Parker Schuh, Kensen Shi, Sasha Tsvyashchenko, Joshua Maynez, Abhishek Rao, Parker Barnes, Yi Tay, Noam Shazeer, Vinodkumar Prabhakaran, Emily Reif, Nan Du, Ben Hutchinson, Reiner Pope, James Bradbury, Jacob Austin, Michael Isard, Guy Gur-Ari, Pengcheng Yin, Toju Duke, Anselm Levskaya, Sanjay Ghemawat, Sunipa Dev, Henryk Michalewski, Xavier Garcia, Vedant Misra, Kevin Robinson, Liam Fedus, Denny Zhou, Daphne Ippolito, David Luan, Hyeontaek Lim, Barret Zoph, Alexander Spiridonov, Ryan Sepassi, David Dohan, Shivani Agrawal, Mark Omernick, Andrew M. Dai, Thanumalayan Sankaranarayanan Pillai, Marie Pellat, Aitor Lewkowycz, Erica Moreira, Rewon Child, Oleksandr Polozov, Katherine Lee, Zongwei Zhou, Xuezhi Wang, Brennan Saeta, Mark Diaz, Orhan Firat, Michele Catasta, Jason Wei, Kathy Meier-Hellstern, Douglas Eck, Jeff Dean, Slav Petrov, and Noah Fiedel. PaLM: Scaling Language Modeling with Pathways, October 2022. URL <http://arxiv.org/abs/2204.02311>. arXiv:2204.02311 [cs].
- Alexander Dunn, John Dagdelen, Nicholas Walker, Sanghoon Lee, Andrew S. Rosen, Gerbrand Ceder, Kristin Persson, and Anubhav Jain. Structured information extraction from complex scientific text with fine-tuned large language models, December 2022. URL <http://arxiv.org/abs/2212.05238>. arXiv:2212.05238 [cond-mat].
- Nathan Frey, Ryan Soklaski, Simon Axelrod, Siddharth Samsi, Rafael Gomez-Bombarelli, Connor Coley, and Vijay Gadepally. Neural Scaling of Deep Chemical Models, May 2022. URL <https://chemrxiv.org/engage/chemrxiv/article-details/627bddd544bdd532395fb4b5>.
- Alex M. Ganose and Anubhav Jain. Robocrystallographer: automated crystal structure text descriptions and analysis. *MRS Communications*, 9(3):874–881, September 2019. ISSN 2159-6867. doi: 10.1557/mrc.2019.94. URL <https://doi.org/10.1557/mrc.2019.94>.
- Sinéad M. Griffin. Origin of correlated isolated flat bands in copper-substituted lead phosphate apatite, July 2023. URL <http://arxiv.org/abs/2307.16892>. arXiv:2307.16892 [cond-mat].
- Nate Gruver, Anuroop Sriram, Andrea Madotto, Andrew Wilson, C. Lawrence Zitnick, and Zachary Ulissi. Fine-Tuned Language Models Generate Stable Inorganic Materials as Text. November 2023. URL <https://openreview.net/forum?id=0r5DE2ZSwJ>.

-
- Tanishq Gupta, Mohd Zaki, N. M. Anoop Krishnan, and Mausam. MatSciBERT: A materials domain language model for text mining and information extraction. *npj Computational Materials*, 8(1):1–11, May 2022. ISSN 2057-3960. doi: 10.1038/s41524-022-00784-w. URL <https://www.nature.com/articles/s41524-022-00784-w>. Number: 1 Publisher: Nature Publishing Group.
- Anubhav Jain, Geoffroy Hautier, Charles J. Moore, Shyue Ping Ong, Christopher C. Fischer, Tim Mueller, Kristin A. Persson, and Gerbrand Ceder. A high-throughput infrastructure for density functional theory calculations. *Computational Materials Science*, 50(8):2295–2310, June 2011. ISSN 0927-0256. doi: 10.1016/j.commatsci.2011.02.023. URL <https://www.sciencedirect.com/science/article/pii/S0927025611001133>.
- Anubhav Jain, Shyue Ping Ong, Geoffroy Hautier, Wei Chen, William Davidson Richards, Stephen Dacek, Shreyas Cholia, Dan Gunter, David Skinner, Gerbrand Ceder, and Kristin A. Persson. Commentary: The Materials Project: A materials genome approach to accelerating materials innovation. *APL Materials*, 1(1):011002, July 2013. ISSN 2166-532X. doi: 10.1063/1.4812323. URL <https://doi.org/10.1063/1.4812323>.
- Nikhil Kandpal, Haikang Deng, Adam Roberts, Eric Wallace, and Colin Raffel. Large Language Models Struggle to Learn Long-Tail Knowledge, July 2023. URL <http://arxiv.org/abs/2211.08411>. arXiv:2211.08411 [cs].
- Olga Kononova, Haoyan Huo, Tanjin He, Ziqin Rong, Tiago Botari, Wenhao Sun, Vahe Tshitoyan, and Gerbrand Ceder. Text-mined dataset of inorganic materials synthesis recipes. *Scientific Data*, 6(1):203, October 2019. ISSN 2052-4463. doi: 10.1038/s41597-019-0224-1. URL <https://www.nature.com/articles/s41597-019-0224-1>. Number: 1 Publisher: Nature Publishing Group.
- G. Kresse and J. Furthmüller. Efficient iterative schemes for ab initio total-energy calculations using a plane-wave basis set. *Physical Review B*, 54(16):11169–11186, October 1996. doi: 10.1103/PhysRevB.54.11169. URL <https://link.aps.org/doi/10.1103/PhysRevB.54.11169>. Publisher: American Physical Society.
- Valérie Laperche, Terry J. Logan, Pranitha Gaddam, and Samuel J. Traina. Effect of Apatite Amendments on Plant Uptake of Lead from Contaminated Soil. *Environmental Science & Technology*, 31(10):2745–2753, October 1997. ISSN 0013-936X. doi: 10.1021/es961011o. URL <https://doi.org/10.1021/es961011o>. Publisher: American Chemical Society.
- Sukbae Lee, Ji-Hoon Kim, and Young-Wan Kwon. The First Room-Temperature Ambient-Pressure Superconductor, July 2023a. URL <http://arxiv.org/abs/2307.12008>. arXiv:2307.12008 [cond-mat].
- Sukbae Lee, Jihoon Kim, Hyun-Tak Kim, Sungyeon Im, SooMin An, and Keun Ho Auh. Superconductor $\text{Pb}_{1-x}\text{Cu}_x(\text{PO}_4)_6\text{O}$ showing levitation at room temperature and atmospheric pressure and mechanism, August 2023b. URL <http://arxiv.org/abs/2307.12037>. arXiv:2307.12037 [cond-mat].
- Patrick Lewis, Ethan Perez, Aleksandra Piktus, Fabio Petroni, Vladimir Karpukhin, Naman Goyal, Heinrich Küttler, Mike Lewis, Wen-tau Yih, Tim Rocktäschel, Sebastian Riedel, and Douwe Kiela. Retrieval-Augmented Generation for Knowledge-Intensive NLP Tasks. In *Advances in Neural Information Processing Systems*, volume 33, pp. 9459–9474. Curran Associates, Inc., 2020. URL <https://proceedings.neurips.cc/paper/2020/hash/6b493230205f780e1bc26945df7481e5-Abstract.html>.
- Patrick Lewis, Ethan Perez, Aleksandra Piktus, Fabio Petroni, Vladimir Karpukhin, Naman Goyal, Heinrich Küttler, Mike Lewis, Wen-tau Yih, Tim Rocktäschel, Sebastian Riedel, and Douwe Kiela. Retrieval-Augmented Generation for Knowledge-Intensive NLP Tasks, April 2021. URL <http://arxiv.org/abs/2005.11401>. arXiv:2005.11401 [cs] version: 4.
- Jun Li, Andrew E. Smith, Peng Jiang, Judith K. Stalick, Arthur W. Sleight, and M. A. Subramanian. True Composition and Structure of Hexagonal “YAlO₃”, Actually Y₃Al₃O₈CO₃. *Inorganic Chemistry*, 54(3):837–844, February 2015. ISSN 0020-1669. doi: 10.1021/ic502027k. URL <https://doi.org/10.1021/ic502027k>. Publisher: American Chemical Society.

-
- Nelson F. Liu, Kevin Lin, John Hewitt, Ashwin Paranjape, Michele Bevilacqua, Fabio Petroni, and Percy Liang. Lost in the Middle: How Language Models Use Long Contexts, November 2023. URL <http://arxiv.org/abs/2307.03172>. arXiv:2307.03172 [cs].
- Alex Mallen, Akari Asai, Victor Zhong, Rajarshi Das, Daniel Khashabi, and Hannaneh Hajishirzi. When Not to Trust Language Models: Investigating Effectiveness of Parametric and Non-Parametric Memories, July 2023. URL <http://arxiv.org/abs/2212.10511>. arXiv:2212.10511 [cs].
- Andrey L. Maximenko and Eugene A. Olevsky. Effective diffusion coefficients in solid-state sintering. *Acta Materialia*, 52(10):2953–2963, June 2004. ISSN 1359-6454. doi: 10.1016/j.actamat.2004.02.042. URL <https://www.sciencedirect.com/science/article/pii/S1359645404001326>.
- Amil Merchant, Simon Batzner, Samuel S. Schoenholz, Muratahan Aykol, Gwooon Cheon, and Ekin Dogus Cubuk. Scaling deep learning for materials discovery. *Nature*, pp. 1–6, November 2023. ISSN 1476-4687. doi: 10.1038/s41586-023-06735-9. URL <https://www.nature.com/articles/s41586-023-06735-9>. Publisher: Nature Publishing Group.
- Brianna L. Musicó, Dustin Gilbert, Thomas Zac Ward, Katharine Page, Easo George, Jiaqiang Yan, David Mandrus, and Veerle Keppens. The emergent field of high entropy oxides: Design, prospects, challenges, and opportunities for tailoring material properties. *APL Materials*, 8(4):040912, April 2020. ISSN 2166-532X. doi: 10.1063/5.0003149. URL <https://doi.org/10.1063/5.0003149>.
- Shyue Ping Ong, William Davidson Richards, Anubhav Jain, Geoffroy Hautier, Michael Kocher, Shreyas Cholia, Dan Gunter, Vincent L. Chevrier, Kristin A. Persson, and Gerbrand Ceder. Python Materials Genomics (pymatgen): A robust, open-source python library for materials analysis. *Computational Materials Science*, 68:314–319, February 2013. ISSN 0927-0256. doi: 10.1016/j.commatsci.2012.10.028. URL <https://www.sciencedirect.com/science/article/pii/S0927025612006295>.
- OpenAI. GPT-4 Technical Report, March 2023. URL <http://arxiv.org/abs/2303.08774>. arXiv:2303.08774 [cs].
- Maciej P. Polak and Dane Morgan. Extracting Accurate Materials Data from Research Papers with Conversational Language Models and Prompt Engineering, June 2023. URL <http://arxiv.org/abs/2303.05352>. arXiv:2303.05352 [cond-mat].
- Alec Radford, Jong Wook Kim, Chris Hallacy, Aditya Ramesh, Gabriel Goh, Sandhini Agarwal, Girish Sastry, Amanda Askell, Pamela Mishkin, Jack Clark, Gretchen Krueger, and Ilya Sutskever. Learning Transferable Visual Models From Natural Language Supervision, February 2021. URL <http://arxiv.org/abs/2103.00020>. arXiv:2103.00020 [cs].
- Janosh Riebesell, T. Wesley Surta, Rhys Goodall, Michael Gaultois, and Alpha A. Lee. Pushing the Pareto front of band gap and permittivity: ML-guided search for dielectric materials, January 2024. URL <http://arxiv.org/abs/2401.05848>. arXiv:2401.05848 [cond-mat, physics:physics].
- Sina J. Semnani, Violet Z. Yao, Heidi C. Zhang, and Monica S. Lam. WikiChat: Stopping the Hallucination of Large Language Model Chatbots by Few-Shot Grounding on Wikipedia, October 2023. URL <http://arxiv.org/abs/2305.14292>. arXiv:2305.14292 [cs].
- Nathan J. Szymanski, Bernardus Rendy, Yuxing Fei, Rishi E. Kumar, Tanjin He, David Milsted, Matthew J. McDermott, Max Gallant, Ekin Dogus Cubuk, Amil Merchant, Haegyeom Kim, Anubhav Jain, Christopher J. Bartel, Kristin Persson, Yan Zeng, and Gerbrand Ceder. An autonomous laboratory for the accelerated synthesis of novel materials. *Nature*, 624(7990):86–91, December 2023. ISSN 1476-4687. doi: 10.1038/s41586-023-06734-w. URL <https://www.nature.com/articles/s41586-023-06734-w>. Number: 7990 Publisher: Nature Publishing Group.

-
- Paul K. Todd, Matthew J. McDermott, Christopher L. Rom, Adam A. Corrao, Jonathan J. Denney, Shyam S. Dwaraknath, Peter G. Khalifah, Kristin A. Persson, and James R. Neilson. Selectivity in Yttrium Manganese Oxide Synthesis via Local Chemical Potentials in Hyperdimensional Phase Space. *Journal of the American Chemical Society*, 143(37):15185–15194, September 2021. ISSN 0002-7863. doi: 10.1021/jacs.1c06229. URL <https://doi.org/10.1021/jacs.1c06229>. Publisher: American Chemical Society.
- Hugo Touvron, Louis Martin, Kevin Stone, Peter Albert, Amjad Almahairi, Yasmine Babaei, Nikolay Bashlykov, Soumya Batra, Prajjwal Bhargava, Shruti Bhosale, Dan Bikel, Lukas Blecher, Cristian Canton Ferrer, Moya Chen, Guillem Cucurull, David Esiobu, Jude Fernandes, Jeremy Fu, Wenyin Fu, Brian Fuller, Cynthia Gao, Vedanuj Goswami, Naman Goyal, Anthony Hartshorn, Saghar Hosseini, Rui Hou, Hakan Inan, Marcin Kardas, Viktor Kerkez, Madian Khabsa, Isabel Kloumann, Artem Korenev, Punit Singh Koura, Marie-Anne Lachaux, Thibaut Lavril, Jenya Lee, Diana Liskovich, Yinghai Lu, Yuning Mao, Xavier Martinet, Todor Mihaylov, Pushkar Mishra, Igor Molybog, Yixin Nie, Andrew Poulton, Jeremy Reizenstein, Rashi Rungta, Kalyan Saladi, Alan Schelten, Ruan Silva, Eric Michael Smith, Ranjan Subramanian, Xiaoqing Ellen Tan, Binh Tang, Ross Taylor, Adina Williams, Jian Xiang Kuan, Puxin Xu, Zheng Yan, Iliyan Zarov, Yuchen Zhang, Angela Fan, Melanie Kambadur, Sharan Narang, Aurelien Rodriguez, Robert Stojnic, Sergey Edunov, and Thomas Scialom. Llama 2: Open Foundation and Fine-Tuned Chat Models, July 2023. URL <http://arxiv.org/abs/2307.09288>. arXiv:2307.09288 [cs].
- Vahe Tshitoyan, John Dagdelen, Leigh Weston, Alexander Dunn, Ziqin Rong, Olga Kononova, Kristin A. Persson, Gerbrand Ceder, and Anubhav Jain. Unsupervised word embeddings capture latent knowledge from materials science literature. *Nature*, 571(7763):95–98, July 2019. ISSN 1476-4687. doi: 10.1038/s41586-019-1335-8. URL <https://www.nature.com/articles/s41586-019-1335-8>. Number: 7763 Publisher: Nature Publishing Group.
- Ashish Vaswani, Noam Shazeer, Niki Parmar, Jakob Uszkoreit, Llion Jones, Aidan N. Gomez, Lukasz Kaiser, and Illia Polosukhin. Attention Is All You Need, August 2023. URL <http://arxiv.org/abs/1706.03762>. arXiv:1706.03762 [cs].
- Weizhi Wang, Li Dong, Hao Cheng, Xiaodong Liu, Xifeng Yan, Jianfeng Gao, and Furu Wei. Augmenting Language Models with Long-Term Memory, June 2023. URL <http://arxiv.org/abs/2306.07174>. arXiv:2306.07174 [cs].
- Jason Wei, Xuezhi Wang, Dale Schuurmans, Maarten Bosma, Brian Ichter, Fei Xia, Ed Chi, Quoc Le, and Denny Zhou. Chain-of-Thought Prompting Elicits Reasoning in Large Language Models, January 2023. URL <http://arxiv.org/abs/2201.11903>. arXiv:2201.11903 [cs].
- Tong Xie, Yuwei Wan, Wei Huang, Yufei Zhou, Yixuan Liu, Qingyuan Linghu, Shaozhou Wang, Chunyu Kit, Clara Grazian, Wenjie Zhang, and Bram Hoex. Large Language Models as Master Key: Unlocking the Secrets of Materials Science with GPT, April 2023. URL <http://arxiv.org/abs/2304.02213>. arXiv:2304.02213 [cs].
- Samuel Yang, Shutong Li, Subhashini Venugopalan, Vahe Tshitoyan, Muratahan Aykol, Amil Merchant, Ekin Cubuk, and Gowoon Cheon. Accurate Prediction of Experimental Band Gaps from Large Language Model-Based Data Extraction. November 2023. URL <https://openreview.net/forum?id=oRKWhmtUG6>.
- Shunyu Yao, Jeffrey Zhao, Dian Yu, Nan Du, Izhak Shafran, Karthik Narasimhan, and Yuan Cao. ReAct: Synergizing Reasoning and Acting in Language Models, March 2023. URL <http://arxiv.org/abs/2210.03629>. arXiv:2210.03629 [cs].
- Claudio Zeni, Robert Pinsler, Daniel Zügner, Andrew Fowler, Matthew Horton, Xiang Fu, Sasha Shysheya, Jonathan Crabbé, Lixin Sun, Jake Smith, Bichlien Nguyen, Hannes Schulz, Sarah Lewis, Chin-Wei Huang, Ziheng Lu, Yichi Zhou, Han Yang, Hongxia Hao, Jielan Li, Ryota Tomioka, and Tian Xie. MatterGen: a generative model for inorganic materials design, January 2024. URL <http://arxiv.org/abs/2312.03687>. arXiv:2312.03687 [cond-mat].
- Lianmin Zheng, Wei-Lin Chiang, Ying Sheng, Siyuan Zhuang, Zhanghao Wu, Yonghao Zhuang, Zi Lin, Zhuohan Li, Dacheng Li, Eric P. Xing, Hao Zhang, Joseph E. Gonzalez, and Ion Stoica. Judging LLM-as-a-Judge with MT-Bench and Chatbot Arena, December 2023a. URL <http://arxiv.org/abs/2306.05685>. arXiv:2306.05685 [cs].

Zhiling Zheng, Oufan Zhang, Christian Borgs, Jennifer T. Chayes, and Omar M. Yaghi. ChatGPT Chemistry Assistant for Text Mining and Prediction of MOF Synthesis. *Journal of the American Chemical Society*, 145(32):18048–18062, August 2023b. ISSN 0002-7863, 1520-5126. doi: 10.1021/jacs.3c05819. URL <http://arxiv.org/abs/2306.11296>. arXiv:2306.11296 [cond-mat, physics:physics].

A PROMPT TEMPLATE

We use the ReAct template `hwchase17/react-multi-input-json` from LangChain Hub (<https://smith.langchain.com/hub/hwchase17/react-json>) as follows:

```
Answer the following questions as best you can. You have access to the following tools:

{tools}

The way you use the tools is by specifying a JSON blob.
Specifically, this JSON should have an 'action' key (with the name of the tool to use) and an
'action_input' key (with the input to the tool going here).

The only values that should be in the "action" field are: {tool_names}

The $JSON_BLOB should only contain a SINGLE action, do NOT return a list of multiple actions.
Here is an example of a valid $JSON_BLOB:

'''
{{
  "action": $TOOL_NAME,
  "action_input": $INPUT
}}
'''

ALWAYS use the following format:

Question: the input question you must answer
Thought: you should always think about what to do
Action:
'''
$JSON_BLOB
'''
Observation: the result of the action
... (this Thought/Action/Observation can repeat N times)
Thought: I now know the final answer
Final Answer: the final answer to the original input question

Begin! Reminder to always use the exact characters 'Final Answer' when responding.
```

The above system prompt message is prepended with the following solicitation to guide the top-level agent:

```
You are a data-aware agent who can consult materials-related data through the Materials
Project (MP) database, arXiv, and Wikipedia. Ask the user to clarify their queries if
needed. Please note that you don't have direct control over MP but through multiple
assistant agents to help you. You need to provide complete context in the input for them
to do their job.
```

B SAMPLE QUESTIONS

Table 3: QA comparison between LLaMP and GPT-3.5.

	Question	Answer	
		LLaMP	GPT-3.5
B3.1	What are the bulk moduli of the following metals: Sc, Ti, V, Cr, Mn, Fe, Co, Ni, Cu, Zn?	<p>The bulk moduli of the metals you asked for are as follows (in GPa): - Scandium (Sc): Voigt = 45.715, Reuss = 45.34, VRH = 45.528 - Titanium (Ti): Voigt = 112.955, Reuss = 112.807, VRH = 112.881 - Vanadium (V): Voigt = 181.232, Reuss = 181.232, VRH = 181.232 - Chromium (Cr): Voigt = 252.155, Reuss = 252.155, VRH = 252.155 - Manganese (Mn): Voigt = 280.959, Reuss = 280.959, VRH = 280.959 - Iron (Fe): Voigt = 296.003, Reuss = 295.207, VRH = 295.605 - Cobalt (Co): Voigt = 200.587, Reuss = 200.587, VRH = 200.587 - Nickel (Ni): Voigt = 197.399, Reuss = 197.29, VRH = 197.345 - Copper (Cu): Voigt = 151.394, Reuss = 151.394, VRH = 151.394 - Zinc (Zn): Voigt = 76.283, Reuss = 95.46, VRH = 85.872</p>	<p>The bulk modulus (K) is a measure of a material's resistance to uniform compression. It is defined as the ratio of the change in pressure to the fractional volume compression. The values for the bulk modulus can vary somewhat depending on the specific conditions and crystallographic structures of the materials. The values provided here are approximate and given in gigapascals (GPa): - Scandium (Sc): 55 GPa - Titanium (Ti): 110 GPa - Vanadium (V): 160 GPa - Chromium (Cr): 160 GPa - Manganese (Mn): 120 GPa - Iron (Fe): 170 GPa - Cobalt (Co): 180 GPa - Nickel (Ni): 180 GPa - Copper (Cu): 140 GPa - Zinc (Zn): 70 GPa These values represent typical bulk moduli for these metals, and actual values may vary depending on factors such as temperature and pressure.</p>
Continued on next page			

Table 3 – continued from previous page

	Question	Answer	
		LLaMP	GPT-3.5
B3.2	What is the full elastic tensor of NaCl?	<p>The elastic tensor for NaCl is available for two different entries on Materials Project. For material 'id 'mp-22851', the elastic tensor in IEEE format is [[76.0, 1.0, 1.0, -0.0, 0.0, -0.0], [1.0, 76.0, 1.0, -0.0, -0.0, 0.0], [1.0, 1.0, 76.0, 0.0, -0.0, -0.0], [-0.0, -0.0, 0.0, -3.0, -0.0, -0.0], [0.0, -0.0, -0.0, -0.0, -3.0, 0.0], [-0.0, 0.0, -0.0, -0.0, 0.0, -3.0]]. For material 'id 'mp-22862', the elastic tensor in IEEE format is [[47.0, 12.0, 12.0, 0.0, -0.0, -0.0], [12.0, 47.0, 12.0, 0.0, -0.0, -0.0], [12.0, 12.0, 47.0, 0.0, 0.0, -0.0], [0.0, 0.0, 0.0, 12.0, -0.0, -0.0], [-0.0, -0.0, 0.0, -0.0, 12.0, 0.0], [-0.0, -0.0, -0.0, 0.0, 12.0]]</p>	<p>The elastic tensor describes the relationship between stress and strain in a material. It is a 4th-rank tensor that characterizes the elastic properties of a crystal. In the case of NaCl (sodium chloride), the elastic tensor is typically represented by a 6x6 matrix.</p> <p>The elastic constants of NaCl can vary slightly depending on the specific conditions and crystallographic orientation. Here is an approximate form of the elastic tensor for NaCl: $C_{11} = 289.2 \text{ GPa}$ $C_{12} = 97.8 \text{ GPa}$ $C_{44} = 81.6 \text{ GPa}$ $C_{13} = C_{14} = C_{15} = C_{16} = C_{23} = C_{24} = C_{25} = C_{26} = 0 \text{ GPa}$</p> <p>Note: The values are given in gigapascals (GPa). The elastic constants C_{ij} represent the components of the elastic tensor. In this case, C_{11}, C_{12}, and C_{44} are the non-zero elastic constants. The off-diagonal terms C_{13}, C_{14}, C_{15}, C_{16}, C_{23}, C_{24}, C_{25}, and C_{26} are typically zero due to cubic symmetry.</p> <p>Keep in mind that these values are approximate, and there may be slight variations depending on the source and the specific conditions under which the measurements were made. Experimental techniques, such as Brillouin scattering or ultrasonic measurements, are often used to determine the elastic constants of materials.</p>
B3.3	What are the bandgaps of the following materials: Si, Ge, and GaAs, GaN, SiC, BN, InSe, MoS2, BaTiO3, CsPbI3? Only look for ground-state bandgaps.	<p>The ground state bandgaps for the requested materials are as follows: Si: 1.12 eV, Ge: 0.66 eV, GaAs: 1.42 eV, GaN: 3.28 eV, SiC: 2.36 eV, BN: 6.4 eV, InSe: 1.26 eV, MoS2: 1.29 eV, BaTiO3: 3.2 eV, CsPbI3: 1.73 eV. Please note that these values are typical for bulk materials and can vary depending on the specific structure and calculation method.</p>	<p>As of my last knowledge update in January 2022, I can provide you with approximate values for the ground state bandgaps of the materials you mentioned. Keep in mind that these values can vary depending on factors like temperature and crystal structure. Additionally, more recent research may have refined these values. Here are the approximate ground state bandgaps in electron volts (eV): Silicon (Si): 1.1 eV Germanium (Ge): 0.67 eV Gallium Arsenide (GaAs): 1.42 eV Gallium Nitride (GaN): 3.4 eV Silicon Carbide (SiC): 3.2 eV (for 4H-SiC) Boron Nitride (BN): 6 eV Indium Selenide (InSe): 1.25 eV Molybdenum Disulfide (MoS2): 1.3 eV (indirect bandgap) Barium Titanate (BaTiO3): 3.2 eV Cesium Lead Iodide (CsPbI3): 1.7 eV Please note that these values are general approximations and may not represent the specific conditions or variations in different forms of these materials. For the most accurate and up-to-date information, I recommend checking recent scientific literature or databases.</p>

Continued on next page

Table 3 – continued from previous page

	Question	Answer	
		LLaMP	GPT-3.5
B3.4	Give me the decomposition enthalpies of the following materials: Ag ₂ O ₃ , MgZn ₂ , GaAs, GaN, SiC, BN, InSe, MoS ₂ , BaTiO ₃ , CsPbI ₃ . If there are multiple values, please give me the largest value.	The maximum decomposition enthalpies for the requested materials are as follows: - Ag ₂ O ₃ : 0.2565836414999989 eV/atom - MgZn ₂ : 0.1356 eV/atom - GaAs: 0.075 eV/atom - GaN: 0.07162 eV/atom - SiC: -0.172 eV/atom - BN: -0.358 eV/atom - InSe: -0.01816 eV/atom - MoS ₂ : 0.267 eV/atom - BaTiO ₃ : 3.055 eV/atom - CsPbI ₃ : 0.017536019000000902 eV/atom Please note that the values for SiC, BN, and InSe are negative, indicating that the decomposition is exothermic. All other values are positive, indicating endothermic decompositions.	The decomposition enthalpies (in kJ/mol) of the following materials are: Ag ₂ O ₃ : -335 MgZn ₂ : -82 GaAs: -317 GaN: -505 SiC: -40 BN: -248 InSe: -125 MoS ₂ : -393 BaTiO ₃ : -112 CsPbI ₃ : -153
B3.5	Give me the formation energies of the following materials: Ag ₂ O ₃ , MgZn ₂ , GaAs, GaN, SiC, BN, InSe, MoS ₂ , BaTiO ₃ , CsPbI ₃ . If there are multiple values, please give me the smallest value.	The smallest formation energies of the materials you asked for are as follows: Ag ₂ O ₃ : -0.3601 eV/atom, MgZn ₂ : -0.1306 eV/atom, GaAs: -0.446 eV/atom, GaN: -0.052 eV/atom, SiC: -0.204 eV/atom, BN: -1.41 eV/atom, InSe: -0.742582154921875 eV/atom, MoS ₂ : -1.202 eV/atom, BaTiO ₃ : -3.493 eV/atom, CsPbI ₃ : -1.296 eV/atom.	Ag ₂ O ₃ : -2.63 eV/atom MgZn ₂ : -0.27 eV/atom GaAs: -4.13 eV/atom GaN: -3.51 eV/atom SiC: -4.98 eV/atom BN: -3.8 eV/atom InSe: -0.89 eV/atom MoS ₂ : -3.31 eV/atom BaTiO ₃ : -4.45 eV/atom CsPbI ₃ : -2.32 eV/atom
Continued on next page			

Table 3 – continued from previous page

	Question	Answer	
		LLaMP	GPT-3.5
B3.6	Give me the decomposition enthalpies of the following materials: Ag ₂ O ₃ , MgZn ₂ , GaAs, GaN, SiC, BN, InSe, MoS ₂ , BaTiO ₃ , CsPbI ₃ . If there are multiple values, please give me the smallest value.	The smallest decomposition enthalpy values for the requested materials are as follows: Ag ₂ O ₃ : 0.01937364808333528 eV/atom, MgZn ₂ : -0.0197 eV/atom, GaAs: -0.446 eV/atom, GaN: -0.05231 eV/atom, SiC: -0.204 eV/atom, BN: -1.41 eV/atom, InSe: -0.06336 eV/atom, MoS ₂ : -0.669 eV/atom, BaTiO ₃ : -0.063 eV/atom, CsPbI ₃ : -0.018602 eV/atom.	The decomposition enthalpies of the materials are as follows: - Ag ₂ O ₃ : -1138.5 kJ/mol - MgZn ₂ : -54.2 kJ/mol - GaAs: -452.2 kJ/mol - GaN: -510.9 kJ/mol - SiC: -2133.6 kJ/mol - BN: -2551.0 kJ/mol - InSe: -209.3 kJ/mol - MoS ₂ : -739.3 kJ/mol - BaTiO ₃ : -393.5 kJ/mol - CsPbI ₃ : -65.3 kJ/mol
B3.7	Give me the energy above hull values of the following materials: Ba ₂ MnSe ₃ , KAlSiO ₄ , LiCuO, H ₈ C ₃ N ₂ O, Dy ₂ ZnS ₄ , Rb ₂ BeF ₄ , K ₉ Fe ₂ S ₇ , Tb ₂ FeC ₄ , ScAlAu, CaCrO ₄ . If there are multiple values, please give me the lowest one.	Here are the lowest energy above hull values for the requested materials: Ba ₂ MnSe ₃ : 0.0 eV/atom KAlSiO ₄ : 0.0 eV/atom LiCuO: 0.0 eV/atom H ₈ C ₃ N ₂ O: 0.0735 eV/atom Dy ₂ ZnS ₄ : 0.00966 eV/atom Rb ₂ BeF ₄ : 0.0 eV/atom K ₉ Fe ₂ S ₇ : 0.0 eV/atom Tb ₂ FeC ₄ : 0.0 eV/atom ScAlAu: 0.0 eV/atom CaCrO ₄ : 0.0 eV/atom. Please note that these are the lowest values found in the Materials Project database and actual values may vary based on different entries.	The energy above hull values for the given materials are as follows: - Ba ₂ MnSe ₃ : 0.0000 eV/atom - KAlSiO ₄ : 0.0000 eV/atom - LiCuO: 0.0000 eV/atom - H ₈ C ₃ N ₂ O: 0.0000 eV/atom - Dy ₂ ZnS ₄ : 0.0000 eV/atom - Rb ₂ BeF ₄ : 0.0000 eV/atom - K ₉ Fe ₂ S ₇ : 0.0000 eV/atom - Tb ₂ FeC ₄ : 0.0000 eV/atom - ScAlAu: 0.0000 eV/atom - CaCrO ₄ : 0.0000 eV/atom

Continued on next page

Table 3 – continued from previous page

	Question	Answer	
		LLaMP	GPT-3.5
B3.8	What are the bandgaps of the following materials: Ba(PdS2)2, FePO4, DyBi2IO4, NaFe(SO4)2, Eu2B5BrO9, Sr5As3H, TlGaS2, AgSbS2, Pr3S3N, LiLaO2. If there are polymorphs, give me only the bandgap of the stable material.	<p>The bandgaps for the materials are:</p> <ul style="list-style-type: none"> - Ba(PdS2)2: 0.779 eV - Most stable FePO4: 2.1932 eV - DyBi2IO4: 1.367 eV - Most stable NaFe(SO4)2: 2.094 eV - Eu2B5BrO9: 0.88 eV - Sr5As3H: 0.676 eV - TlGaS2: 1.7885 eV - Most stable AgSbS2: 1.372 eV - Pr3S3N: 1.15 eV - Most stable LiLaO2: 3.7336 eV <p>Please note that these values are obtained from the Materials Project database and might be different in experimental results due to various factors.</p>	<p>I don't have real-time data access, and my training only includes information available up to January 2022. As a result, I may not have specific bandgap values for the materials you mentioned. However, I can provide you with general information about some of these materials and their known properties up to my last update:</p> <p>Ba(PdS2)2: I don't have specific bandgap information for this compound. The bandgap may depend on factors such as crystal structure and synthesis conditions.</p> <p>FePO4: Iron(II) phosphate, known as ferrous phosphate, typically has a bandgap in the range of 2.5-3.0 eV.</p> <p>DyBi2IO4: Dysprosium bismuth iodate. I don't have specific bandgap information for this compound.</p> <p>NaFe(SO4)2: Sodium iron sulfate. I don't have specific bandgap information for this compound.</p> <p>Eu2B5BrO9: Europium borate bromate. I don't have specific bandgap information for this compound.</p> <p>Sr5As3H: Strontium arsenide hydride. I don't have specific bandgap information for this compound.</p> <p>TlGaS2: Thallium gallium sulfide. I don't have specific bandgap information for this compound.</p> <p>AgSbS2: Silver antimony sulfide. This material is a semiconductor with a bandgap typically around 1.5-2.0 eV.</p> <p>Pr3S3N: Praseodymium sulfide nitride. I don't have specific bandgap information for this compound.</p> <p>LiLaO2: Lithium lanthanum oxide. I don't have specific bandgap information for this compound.</p> <p>The most stable structure for each material can vary based on synthesis conditions and other factors. For accurate and up-to-date bandgap values and structural information, you may want to consult recent scientific literature or databases that specialize in material properties.</p>

Continued on next page

Table 3 – continued from previous page

	Question	Answer	
		LLaMP	GPT-3.5
B3.9	How to synthesize YMnO ₃ ?	<p>To synthesize YMnO₃, a solid-state reaction method can be employed. Here is a summarized procedure based on the synthesis details provided in the literature with DOI: 10.1021/ic502027k:</p> <ol style="list-style-type: none"> 1. Dissolve Y(NO₃)₃·6H₂O, Mn(NO₃)₂·4H₂O, and a source of [OH⁻] in water to create a homogeneous solution. 2. Add citric acid to the solution to act as a mixing media. 3. Heat the mixture at 250°C for 2 hours to achieve pre-calcination. 4. Finally, heat the pre-calcined mixture at a temperature range of 700°C to 930°C for 10 to 18 hours in an air atmosphere to form YMnO₃. 	<p>Synthesizing YMnO₃ (yttrium manganite) typically involves the solid-state reaction method. Please note that the details may vary depending on the specific conditions and equipment available in your laboratory. Here's a general procedure:</p> <p>Materials: Yttrium oxide (Y₂O₃) Manganese oxide (MnO₂ or Mn₂O₃) High-purity manganese carbonate (MnCO₃) Lithium carbonate (Li₂CO₃) or lithium hydroxide (LiOH) Crucible and pestle High-temperature furnace Mortar and pestle Platinum crucible or alumina crucible</p> <p>Procedure:</p> <p>Step 1: Weighing the Precursors Weigh the appropriate amounts of yttrium oxide (Y₂O₃), manganese oxide (MnO₂ or Mn₂O₃), and lithium carbonate (Li₂CO₃) or lithium hydroxide (LiOH) according to the stoichiometric ratio of YMnO₃.</p> <p>Step 2: Mixing the Powders 2. Grind the powders thoroughly in a mortar and pestle to ensure a homogeneous mixture.</p> <p>Step 3: Heating 3. Place the mixed powder in a crucible or alumina crucible. Heat the mixture in a high-temperature furnace. The specific temperature and heating rate depend on the exact synthesis conditions, but a typical range is 800-1100°C.</p> <p>Step 4: Sintering 5. Hold the mixture at the target temperature for a specific duration (several hours) to allow for sintering and the formation of YMnO₃.</p> <p>Step 5: Cooling 6. Slowly cool the sample to room temperature to avoid thermal stress.</p> <p>Step 6: Characterization 7. Characterize the synthesized YMnO₃ using techniques such as X-ray diffraction (XRD), scanning electron microscopy (SEM), and energy-dispersive X-ray spectroscopy (EDS) to confirm the desired phase and composition.</p> <p>Notes: The choice of manganese precursor (MnO₂ or Mn₂O₃) and lithium source (carbonate or hydroxide) can impact the synthesis process and may require optimization. It's crucial to use high-purity starting materials to avoid impurities in the final product. The specific temperatures and times mentioned are general guidelines and may need to be adjusted based on the equipment and conditions in your laboratory. Always follow safety protocols when working with high temperatures and potentially hazardous materials. This is a simplified overview, and you should consult relevant literature and adapt the procedure based on your specific requirements and equipment.</p>

Continued on next page

Table 3 – continued from previous page

	Question	Answer	
		LLaMP	GPT-3.5
B3.10	How to synthesis LiFePO ₄ ? Please provide a detailed step-by-step procedure and the reference.	<p>LiFePO₄ can be synthesized using various methods. One method involves a high-temperature solid-state synthesis using precursors such as Fe₂O₃, LiOH, and NH₄H₂PO₄. The precursors are mixed and heated at temperatures up to 850°C for several days. Another method uses a sol-gel combustion approach with precursors like FePO₄ and Li₂CO₃, where the mixture is calcined at 700°C in a nitrogen atmosphere. For detailed procedures, please refer to the following scientific literature:</p> <ol style="list-style-type: none"> 1. High-temperature solid-state synthesis - DOI: 10.1021/jp407510h 2. Ion-exchange method - DOI: 10.1021/cm402617b 3. Solution method - DOI: 10.1021/jp306936t 4. Solid-state reactions - DOI: 10.1021/cm303259j 5. Sol-gel combustion method - DOI: 10.1007/s10853-011-6139-7 	<p>Synthesizing LiFePO₄ (lithium iron phosphate) typically involves a solid-state reaction method. Below is a step-by-step procedure for synthesizing LiFePO₄:</p> <p>Materials: - Lithium carbonate (Li₂CO₃) - Iron (II) acetate (Fe(CH₃COO)₂) - Ammonium dihydrogen phosphate (NH₄H₂PO₄) - Phosphoric acid (H₃PO₄) - Deionized water - Ethanol - Mortar and pestle - Crucible - Furnace</p> <p>Procedure: 1. Weigh out the appropriate amounts of lithium carbonate (Li₂CO₃) and iron (II) acetate (Fe(CH₃COO)₂) in a 1:1 molar ratio. For example, if you want to synthesize 1 mole of LiFePO₄, you would weigh out 74.55 grams of Li₂CO₃ and 173.93 grams of Fe(CH₃COO)₂.</p> <ol style="list-style-type: none"> 2. Grind the lithium carbonate and iron (II) acetate together using a mortar and pestle to ensure a homogenous mixture. 3. Weigh out the appropriate amount of ammonium dihydrogen phosphate (NH₄H₂PO₄) and add it to the lithium carbonate and iron (II) acetate mixture in a 1:1 molar ratio. For example, if you are synthesizing 1 mole of LiFePO₄, you would weigh out 122.00 grams of NH₄H₂PO₄. 4. Add a few drops of phosphoric acid (H₃PO₄) to the mixture to adjust the pH to around 7. This will help in the formation of LiFePO₄. 5. Add a small amount of deionized water to the mixture and mix it thoroughly to form a slurry. 6. Slowly evaporate the water from the slurry by placing it on a hot plate or in a furnace at a low temperature. 7. Once the water has evaporated, heat the mixture in a crucible in a furnace at around 600-700°C for several hours to initiate the solid-state reaction and form LiFePO₄. 8. After the reaction is complete, allow the crucible to cool and collect the LiFePO₄ powder. 9. Wash the LiFePO₄ powder with ethanol to remove any impurities and then dry it in a desiccator. <p>Reference: P. G. Bruce, B. Scrosati, J.-M. Tarascon, "Nanomaterials for Rechargeable Lithium Batteries," <i>Angew. Chem. Int. Ed.</i> 2008, 47, 2930-2946. DOI: 10.1002/anie.200702505.</p>

Continued on next page

Table 3 – continued from previous page

	Question	Answer	
		LLaMP	GPT-3.5
B3.11	Could you insert one Li atom at the tetrahedral interstitial site in diamond cubic Si? Pull out the most stable DC Si structure from MP directly in JSON string, modify the retrieved structure directly, and give me the final pymatgen structure as a JSON string.	<p>The final structure after inserting a Li atom at the tetrahedral interstitial site in the diamond cubic Si structure is as follows:</p> <pre>{'module': 'pymatgen.core. structure', '@class': ' Structure', 'charge': 0, ' lattice': {'matrix': [[3.333573, 0.0, 1.924639], [1.111191, 3.142924, 1.924639], [0.0, 0.0, 3.849278]], 'pbc': [True, True, True], 'a': 3.8492784033699095, 'b': 3.8492794116013456, 'c': 3.849278, 'alpha': 60.00001213094421, 'beta': 60.00000346645984, 'gamma': 60.00001097545789, 'volume': 40.32952684741405}, ' properties': {}, 'sites': [{' species': [{'element': 'Si', 'occu': 1}], 'abc': [0.875, 0.875, 0.875], 'xyz': [3.8891685, 2.7500584999999997, 6.7362365], 'properties': {' magmom': -0.0}, 'label': 'Si '}, {'species': [{'element': 'Si', 'occu': 1}], 'abc': [0.125, 0.125, 0.125], 'xyz': [0.5555955, 0.3928655, 0.9623195], 'properties': {' magmom': -0.0}, 'label': 'Si '}, {'species': [{'element': 'Li', 'occu': 1}], 'abc': [0.5, 0.5, 0.5], 'xyz': [2.222382, 1.571462, 1.924639], 'properties': {}, 'label': 'Li'}}</pre>	<p>Here's the JSON string for the most stable diamond cubic Si structure retrieved directly from MP:</p> <pre>```json {'sites': [{'species': [{'element': 'Si', 'occu': 1}], 'abc': [0, 0, 0], 'xyz': [0, 0, 0], 'label': 'Si', 'properties': {}}, {'species': [{'element': 'Si', 'occu': 1}], 'abc': [0.25, 0.25, 0.25], 'xyz': [0.178, 0.178, 0.178], 'label': 'Si', ' properties': {}}, 'lattice': {'matrix': [[3.866002, 0, 2.243049], [3.866002, 3.866002, 0], [0, 3.866002, 2.243049]], 'a': 5.431, 'b': 5.431, 'c': 5.431, 'alpha': 109.471219, 'beta': 109.471219, 'gamma': 109.471219, 'volume': 129.584354898}, 'properties': {'space_group': {'number': 227, 'source': 'spglib', 'symbol': 'Fd-3m'}}} ```</pre> <p>Now, let's insert one Li atom at the tetrahedral interstitial site in this diamond cubic Si structure and retrieve the final pymatgen structure as a JSON string:</p> <pre>```json {'sites': [{'species': [{'element': 'Si', 'occu': 1}], 'abc': [0, 0, 0], 'xyz': [0, 0, 0], 'label': 'Si', 'properties': {}}, {'species': [{'element': 'Si', 'occu': 1}], 'abc': [0.25, 0.25, 0.25], 'xyz': [0.178, 0.178, 0.178], 'label': 'Si', 'properties': {}}, {'species': [{'element': 'Li', 'occu': 1}], 'abc': [0.5, 0.5, 0.5], 'xyz': [0.5, 0.5, 0.5], 'label': 'Li', 'properties': {}}, 'lattice': {'matrix': [[3.866002, 0, 2.243049], [3.866002, 3.866002, 0], [0, 3.866002, 2.243049]], 'a': 5.431, 'b': 5.431, 'c': 5.431, 'alpha': 109.471219, 'beta': 109.471219, 'gamma': 109.471219, 'volume': 129.584354898}, 'properties': {'space_group': {'number': 227, 'source': 'spglib', 'symbol': 'Fd-3m'}}} ```</pre>